Available online at www.sciencedirect.com
SCIENCE DIRECT®
ELSEVIER
International Journal of Solids and Structures 43 (2006) 2146–2159
INTERNATIONAL JOURNAL OF SOLIDS and STRUCTURES
www.elsevier.com/locate/ijsolstr

Effect of the nonlinear pre-buckling state on the bifurcation point of conical shells

Mahmood Jabareen, Izhak Sheinman *

Faculty of Civil and Environmental Engineering, Technion—Israel Institute of Technology, Haifa 32000, Israel

Received 16 December 2004; received in revised form 22 May 2005
Available online 20 July 2005

Abstract

The effect of pre-buckling nonlinearity on the bifurcation point of a conical shell is examined on the basis of three shell theories: Donnell's, Sanders' and Timoshenko's. The eigenvalue problem is solved iteratively about the nonlinear equilibrium state up to the bifurcation point. A new algorithm is presented for the real buckling behavior, dispensing with the need to cover the entire nonlinear pattern. This algorithm is very important for structures characterized by a softening process, in which the pre-buckling nonlinearity depresses the buckling level relative to the classical one.

The procedure involves nonlinear partial differential equations, which are separated into two sets (using the perturbation technique) for the pre-buckling and buckling states, respectively and solved with the variable expanded in Fourier series in the circumferential direction, and by finite differences in the axial direction. A general computer code was developed and used in studying the effect of the pre-buckling nonlinearity on the buckling level, of the shell under axial compression, in the context of the three shell theories.

Keywords: Conical shell; Bifurcation point; Buckling load; Nonlinear analysis; Shell theories

1. Introduction

Loss of stability by buckling in shell-like structures is one of the most important and crucial failure phenomena. Treatment of the buckling process as a linear one in this context has been questioned due to the discrepancies observed between theoretical predictions and experimental results. The first reason for these discrepancies is the fact that the structures in question are subjected to considerable nonlinear pre-buckling deformation; consequently, the linear approach is unsuitable for predicting their stability. The second is the

* Corresponding author. Tel.: +972 4829 3042; fax: +972 4829 5697.
E-mail address: cvrnrsh@techunix.technion.ac.il (I. Sheinman).

0020-7683/$ - see front matter © 2005 Elsevier Ltd. All rights reserved.
doi:10.1016/j.ijsolstr.2005.05.024

fact that the load capacity of such structures is strongly affected by the initial imperfection pattern. Accordingly, two main approaches are available for our purpose: (I) consideration of the sensitivity to imperfection, see e.g., Goldfeld et al. (2003); (II) determination of the real buckling load while dispensing with the need to cover the entire nonlinear equilibrium path.

The present paper is concerned with the second approach. For this purpose the conical shell is chosen as a representative structure for the entire range of degree of nonlinearity. Namely, cylindrical shell (conical with vertex half-angle ($\alpha = 0°$)) characterized by high nonlinearity, and annular plate ($\alpha = 90°$) characterized by very low nonlinearity. By varying the cone vertex half-angle (α) conclusions can be drawn for the entire range of nonlinearity level.

While the linear stability (with the nonlinear pre-buckling deformation disregarded) of cylindrical and conical shells was extensively studied, its nonlinear counterpart has so far, to the best of the authors' knowledge, attracted less interest. Seide (1956) was the first to derive the critical buckling load for an axisymmetric mode in a conical shell. Singer (1965) also used the asymmetric buckling mode and obtained the same buckling load as Seide. The effect of the four possible in-plane boundary conditions on the buckling behavior of a conical shell under axial compression was studied by Singer (1962) and by Baruch et al. (1970). Pariatmono and Chryssanthopoulos (1995) and Spagnoli (2003) showed that at a certain aspect ratio of a conical shell, different buckling modes correspond to the same value of critical buckling. Tong (1994) suggested a simple formula for the critical buckling loads of laminated conical shells, based on Seide's (1956) and assuming constant stiffness. Recently, Goldfeld and Arbocz (2004) studied the influence of variation of the stiffness coefficients on the buckling behavior of laminated conical shells.

So far most of the relevant studies have been limited to the simplified theoretical treatment assuming membrane-like or linear pre-buckling. There are, however, a few studies where the influence of the pre-buckling state is taken into account. Brush (1980) considered the effect of pre-buckling rotation in a cylindrical shell and improved accordingly the buckling load obtained without it. Famili (1965) studied the asymmetric behavior of truncated and complete conical shells under uniform hydrostatic pressure, also taking into account the large deformation in the pre-buckling state. Zhang (1993) studied, in the same manner, the buckling and initial post-buckling behavior, with considering the nonlinear pre-buckling behavior, under axial compression and hydrostatic pressure. The limitation in Famili's and Zhang's works is the assumption of an axisymmetric pre-buckling solution and recourse to WF formulation (where W is the normal displacement and F is the Airy stress function), which may yield inaccurate results as was shown later in Sheinman and Goldfeld (2001). For general structures, using the finite-element technique, Brendel and Ramm (1980) devised an improved scheme for prediction of the critical load, with additional linear buckling analyses carried out at a number of intermediate load levels preceding instability. Chang and Chen (1986) proposed a scheme for prediction the real buckling load based on combination of the linear and nonlinear analyses, and with disregarding the stiffness terms which are quadratically dependent on the generalized displacement.

While extensive literature is devoted to processes characterized by a limit point, very few works cover the entire nonlinearity range. From the analytical point of view, two approaches are used in investigating the effect of pre-buckling nonlinearity: (I) the full nonlinear analysis which yields an exact prediction of the nonlinear bifurcation point by finding the intersection of two (or more) equilibrium paths; this approach entails a heavy computational effort; (II) the eigenvalue approach, focusing on the nonlinear equilibrium state. The eigenvalue problem is solved iteratively until the eigenvalue for the current load equals unity, thus yielding the stiffness and geometric matrices right at the bifurcation point; this approach is substantially more effective and computationally cheaper.

The primary objective of the present paper is a new algorithm for the real buckling load dispensing with the need to cover the entire nonlinear behavior. Due to the significant differences between the various shell theories as regard the classical buckling load (Sheinman and Goldfeld, 2001), the sensitivity to imperfection (Sheinman and Goldfeld, 2003) and the nonlinear behavior till the limit point (Simitses et al., 1985),

depending on the cone aspect ratio—the suggested algorithm is examined for three theories: approximational (Donnell's, 1933), accurate (Sanders' , 1963) and more accurate (Timoshenko and Gere's, 1961).

The nonlinear equilibrium differential equations are derived for axial compression, torsion and hydrostatic pressure—with the aid of the variational principle based on the kinematic relations of the theories. The perturbation technique is used to separate the nonlinear equations into nonlinear pre-buckling and linear buckling sets. These two sets are solved through expansion of the unknown functions (u, v and w) in Fourier series in the circumferential direction and by finite differences in the axial direction. The Galerkin procedure is then applied for minimizing the error due to truncation of the Fourier series. A general computer code was developed and used in the parametric study.

The parametric study of the shells under axial compression reveals that the nonlinear pre-buckling deformations have a significant effect on the real buckling state.

2. Mathematical formulation

2.1. Kinematics

The analytical model is based on the Kirchhoff–Love hypothesis, whereby the strains at any material point (x,θ,z) (x being the coordinate in the meridional direction, θ the circumferential angle and z the outward normal, Fig. 1), reads

$$\{\varepsilon(x,\theta,z)\} = \{\bar{\varepsilon}(x,\theta)\} + z\{\kappa(x,\theta)\}, \tag{1}$$

where $\{\bar{\varepsilon}\}$ and $\{\kappa\}$ are the nonlinear membrane tensor and the change of curvature tensor of the reference surface, respectively. Let u, v and w (functions of x and θ) be the components of the displacements of the shell surface in the x, θ and z directions, respectively. Under the Donnell, Sanders and Timoshenko kinematic approaches, the strain–displacement relations read

$$\begin{aligned}
\{\bar{\varepsilon}\} &= \begin{Bmatrix} \bar{\varepsilon}_{xx} \\ \bar{\varepsilon}_{\theta\theta} \\ \bar{\gamma}_{x\theta} \end{Bmatrix} = \begin{Bmatrix} e_{xx} + \frac{1}{2}\phi_x^2 + \delta_2 \frac{(e_{x\theta} - \phi)^2}{2} \\ e_{\theta\theta} + \frac{1}{2}\phi_\theta^2 \\ 2e_{x\theta} + \phi_x \phi_\theta \end{Bmatrix}, \\
\{\kappa\} &= \begin{Bmatrix} \kappa_{xx} \\ \kappa_{\theta\theta} \\ \kappa_{x\theta} \end{Bmatrix} = \begin{Bmatrix} \phi_{x,x} \\ \frac{\phi_{\theta,\theta}}{r(x)} + \frac{\sin(\alpha)}{r(x)}\phi_x \\ \frac{1}{2}\left(\frac{\phi_{x,\theta}}{r(x)} + \phi_{\theta,x} - \frac{\sin(\alpha)}{r(x)}\phi_\theta\right) \end{Bmatrix},
\end{aligned} \tag{2}$$

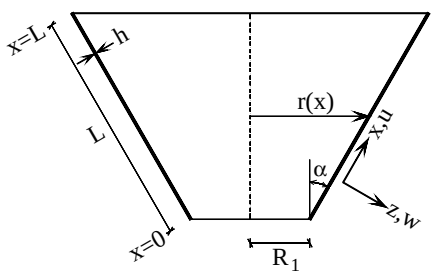

Fig. 1. Geometry and sign convention for coordinates and displacements.

where $(\cdot)_{,x}$ and $(\cdot)_{,\theta}$ denote the derivatives with respect to the axial and circumferential coordinate, respectively, e_{xx}, $e_{\theta\theta}$ and $e_{x\theta}$ are the linear membrane strains; ϕ_x, ϕ_θ are the rotations about the axes of the middle surface, ϕ is the rotation about the normal to the surface, and α is the cone vertex half-angle:

$$\begin{aligned}
e_{xx} &= u_{,x},\\
e_{\theta\theta} &= \frac{v_{,\theta}}{r(x)} + \frac{\cos(\alpha)}{r(x)} w + \frac{\sin(\alpha)}{r(x)} u,\\
e_{x\theta} &= \frac{u_{,\theta}}{2r(x)} + \frac{v_{,x}}{2} - \frac{\sin(\alpha)}{2r(x)} v,\\
\phi &= \frac{u_{,\theta}}{2r(x)} - \frac{v_{,x}}{2} - \frac{\sin(\alpha)}{2r(x)} v,\\
\phi_x &= -w_{,x},\\
\phi_\theta &= \frac{-w_{,\theta} + \delta_1 \cos(\alpha) v}{r(x)},\\
r(x) &= R_1 + x\sin(\alpha),
\end{aligned} \tag{3}$$

R_1 is defined in Fig. 1.

The parameters δ_1 and δ_2 are introduced as follows:

$\delta_1 = \delta_2 = 0$ for Donnell's theory;
$\delta_1 = 1$, $\delta_2 = 0$ for Sanders' theory;
$\delta_1 = \delta_2 = 1$ for Timoshenko's theory.

2.2. Constitutive relations

For an isotropic conical shell, the constitutive relations read

$$\begin{Bmatrix} \{N\} \\ \{M\} \end{Bmatrix} = \begin{bmatrix} [A] & [0] \\ [0] & [D] \end{bmatrix} \begin{Bmatrix} \{\bar{\varepsilon}\} \\ \{\kappa\} \end{Bmatrix}, \tag{4}$$

$\{N\} = \{N_{xx}, N_{\theta\theta}, N_{x\theta}\}^{\mathrm{T}}$ and $\{M\} = \{M_{xx}, M_{\theta\theta}, M_{x\theta}\}^{\mathrm{T}}$ being the resultant membrane forces and bending moments. The elastic matrices are given by

$$\begin{aligned}
[A] &= \frac{Eh}{1-v^2} \begin{bmatrix} 1 & v & 0 \\ v & 1 & 0 \\ 0 & 0 & \dfrac{1-v}{2} \end{bmatrix},\\
[D] &= \frac{Eh^3}{12(1-v^2)} \begin{bmatrix} 1 & v & 0 \\ v & 1 & 0 \\ 0 & 0 & 1-v \end{bmatrix},
\end{aligned} \tag{5}$$

where E, v and h are the modulus of elasticity, Poisson's ratio and shell's thickness, respectively.

2.3. Equilibrium equations

The equilibrium equations and the appropriate boundary conditions are derived from the stationary of total potential energy:

$$\delta\pi = \int_A [N_{xx}\delta\bar{\varepsilon}_{xx} + N_{\theta\theta}\delta\bar{\varepsilon}_{\theta\theta} + N_{x\theta}\delta\bar{\gamma}_{x\theta} + M_{xx}\delta\kappa_{xx} + M_{\theta\theta}\delta\kappa_{\theta\theta} + 2M_{x\theta}\delta\kappa_{x\theta} - q_u\delta u - q_v\delta v - q_w\delta w]\,\mathrm{d}A = 0, \tag{6}$$

where q_u, q_v and q_w are the external distributed loading in the axial, circumferential and normal directions, respectively. With Eqs. (2) substituted in Eq. (6), application of Gauss's theorem yields the following nonlinear equilibrium equations:

$$\begin{aligned}
&N_{xx,x}+\frac{N_{x\theta,\theta}}{r(x)}+\frac{\sin(\alpha)}{r(x)}[N_{xx}-N_{\theta\theta}]+q_u=0,\\
&\frac{N_{\theta\theta,\theta}}{r(x)}+N_{x\theta,x}+2\frac{\sin(\alpha)}{r(x)}N_{x\theta}+\delta_1\frac{\cos(\alpha)}{r(x)}\left[-N_{\theta\theta}\phi_\theta-N_{x\theta}\phi_x+\frac{M_{\theta\theta,\theta}}{r(x)}+M_{x\theta,x}+2\frac{\sin(\alpha)}{r(x)}M_{x\theta}\right]\\
&\quad+\delta_2\frac{[r(x)N_{xx}(e_{x\theta}-\phi)]_{,x}}{r(x)}+q_v=0,\\
&M_{xx,xx}+\frac{2M_{x\theta,x\theta}}{r(x)}+\frac{M_{\theta\theta,\theta\theta}}{r^2(x)}-\frac{\cos(\alpha)}{r(x)}N_{\theta\theta}+\frac{\sin(\alpha)}{r(x)}\left[2M_{xx,x}-M_{\theta\theta,x}+2\frac{M_{x\theta,\theta}}{r(x)}\right]\\
&\quad-\frac{1}{r(x)}[r(x)N_{xx}\phi_x+r(x)N_{x\theta}\phi_\theta]_{,x}-\frac{1}{r(x)}[N_{x\theta}\phi_x+N_{\theta\theta}\phi_\theta]_{,\theta}+q_w=0
\end{aligned}\tag{7}$$

with the following appropriate boundary conditions:

$$\begin{aligned}
&N_{xx}\quad\text{or } u,\\
&N_{x\theta}+\delta_1\frac{\cos(\alpha)}{r(x)}M_{x\theta}+\delta_2N_{xx}(e_{x\theta}-\phi)\quad\text{or } v,\\
&M_{xx,x}+\frac{2M_{x\theta,\theta}}{r(x)}+\frac{\sin(\alpha)}{r(x)}[M_{xx}-M_{\theta\theta}]-N_{xx}\phi_x-N_{x\theta}\phi_\theta\quad\text{or } w,\\
&M_{xx}\quad\text{or } w_{,x}.
\end{aligned}\tag{8}$$

Using the kinematic and constitutive relations (Eqs. (2) and (4)), the equilibrium equations and the appropriate boundary conditions (Eqs. (7) and (8)) can be written in terms of the displacement components as

$$\phi_p(u,v,w)=0,\quad p=1,2,3,\tag{9}$$

ϕ_p can be written in terms of differential operators:

$$\begin{aligned}
&L_p^1(u)+L_p^2(v)+L_p^3(w)+L_p^4(u,v)+L_p^5(u,w)+L_p^6(v,v)+L_p^7(v,w)+L_p^8(w,w)+L_p^9(v,v,v)\\
&\quad+L_p^{10}(v,v,w)+L_p^{11}(v,w,w)+L_p^{12}(w,w,w)+q_p=0,\quad p=1,2,3,
\end{aligned}\tag{10}$$

where $L_p^e(Q), L_p^e(Q,S)$, and $L_p^e(Q,S,T)$ are the linear, quadratic and cubic differential operators (Sheinman and Goldfeld, 2001):

$$\begin{aligned}
L_p^e(Q)&=\sum_{i=0}^{4}\sum_{j=0}^{4-i}\mathfrak{R}_{ij}^{p,e}\frac{\partial^{(i+j)}Q}{\partial x^{(i)}\partial\theta^{(j)}},\\
L_p^e(Q,S)&=\sum_{i=0}^{3}\sum_{j=0}^{3-i}\sum_{k=0}^{3}\sum_{\ell=0}^{\ell-k}\mathfrak{R}_{ijk\ell}^{p,e}\frac{\partial^{(i+j)}Q}{\partial x^{(i)}\partial\theta^{(j)}}\frac{\partial^{(k+\ell)}S}{\partial x^{(k)}\partial\theta^{(\ell)}},\\
L_p^e(Q,S,T)&=\sum_{i=0}^{2}\sum_{j=0}^{2-i}\sum_{k=0}^{2}\sum_{\ell=0}^{2-k}\sum_{m=0}^{2}\sum_{n=0}^{2-m}\mathfrak{R}_{ijk\ell mn}^{p,e}\frac{\partial^{(i+j)}Q}{\partial x^{(i)}\partial\theta^{(j)}}\frac{\partial^{(k+\ell)}S}{\partial x^{(k)}\partial\theta^{(\ell)}}\frac{\partial^{(m+n)}T}{\partial x^{(m)}\partial\theta^{(n)}},
\end{aligned}\tag{11}$$

$\mathfrak{R}^{p,e}_{ij}$, $\mathfrak{R}^{p,e}_{ijk\ell}$, and $\mathfrak{R}^{p,e}_{ijk\ell mn}$ are coefficients of the elastic parameters (A_{ij} and D_{ij}), the radius $r(x)$ and the parameters δ_1 and δ_2. The boundary conditions (Eqs. (8)), are written in a similar way. This form of differential operators is especially suitable for symbolic programming.

3. Solution procedure

The pre-buckling and buckling equations are obtained by using the perturbation technique:

$$\begin{Bmatrix} u \\ v \\ w \end{Bmatrix} = \begin{Bmatrix} u^{(0)} \\ v^{(0)} \\ w^{(0)} \end{Bmatrix} + \xi \begin{Bmatrix} u^{(1)} \\ v^{(1)} \\ w^{(1)} \end{Bmatrix} + \cdots \tag{12}$$

The superscript (0) and (1) refer to the pre-buckling and buckling states, respectively. Substitution of Eq. (12) in Eq. (9) yields

$$\phi^0_p(u^{(0)}, v^{(0)}, w^{(0)}) + \xi \phi^1_p(u^{(0)}, v^{(0)}, w^{(0)}, u^{(1)}, v^{(1)}, w^{(1)}) + \cdots = 0, \quad p = 1, 2, 3, \tag{13}$$

where the first expression refers to the pre-buckling equations, given by

$$\begin{aligned} \phi^0_p(u^{(0)}, v^{(0)}, w^{(0)}) = {} & L^1_p(u^{(0)}) + L^2_p(v^{(0)}) + L^3_p(w^{(0)}) + L^4_p(u^{(0)}, v^{(0)}) + L^5_p(u^{(0)}, w^{(0)}) + L^6_p(v^{(0)}, v^{(0)}) \\ & + L^7_p(v^{(0)}, w^{(0)}) + L^8_p(w^{(0)}, w^{(0)}) + L^9_p(v^{(0)}, v^{(0)}, v^{(0)}) + L^{10}_p(v^{(0)}, v^{(0)}, w^{(0)}) \\ & + L^{11}_p(v^{(0)}, w^{(0)}, w^{(0)}) + L^{12}_p(w^{(0)}, w^{(0)}, w^{(0)}) + q_p = 0, \quad p = 1, 2, 3 \end{aligned} \tag{14}$$

and the second expression refers to the buckling equations, given by

$$\begin{aligned} & \phi^1_p(u^{(0)}, v^{(0)}, w^{(0)}, u^{(1)}, v^{(1)}, w^{(1)}) \\ & = L^1_p(u^{(1)}) + L^2_p(v^{(1)}) + L^3_p(w^{(1)}) + L^4_p(u^{(1)}, v^{(0)}) + L^4_p(u^{(0)}, v^{(1)}) + L^5_p(u^{(1)}, w^{(0)}) + L^5_p(u^{(0)}, w^{(1)}) \\ & \quad + L^6_p(v^{(1)}, v^{(0)}) + L^6_p(v^{(0)}, v^{(1)}) + L^7_p(v^{(1)}, w^{(0)}) + L^7_p(v^{(0)}, w^{(1)}) + L^8_p(w^{(1)}, w^{(0)}) + L^8_p(w^{(0)}, w^{(1)}) \\ & \quad + L^9_p(v^{(1)}, v^{(0)}, v^{(0)}) + L^9_p(v^{(0)}, v^{(1)}, v^{(0)}) + L^9_p(v^{(0)}, v^{(0)}, v^{(1)}) + L^{10}_p(v^{(1)}, v^{(0)}, w^{(0)}) + L^{10}_p(v^{(0)}, v^{(1)}, w^{(0)}) \\ & \quad + L^{10}_p(v^{(0)}, v^{(0)}, w^{(1)}) + L^{11}_p(v^{(1)}, w^{(0)}, w^{(0)}) + L^{11}_p(v^{(0)}, w^{(1)}, w^{(0)}) + L^{11}_p(v^{(0)}, w^{(0)}, w^{(1)}) \\ & \quad + L^{12}_p(w^{(1)}, w^{(0)}, w^{(0)}) + L^{12}_p(w^{(0)}, w^{(1)}, w^{(0)}) + L^{12}_p(w^{(0)}, w^{(0)}, w^{(1)}) = 0, \quad p = 1, 2, 3. \end{aligned} \tag{15}$$

The two sets are partial differential equations, and reduce to one of ordinary differential equations by separation of the variables into truncated Fourier series as

$$\begin{Bmatrix} u^{(0)}(x,\theta) \\ v^{(0)}(x,\theta) \\ w^{(0)}(x,\theta) \\ u^{(1)}(x,\theta) \\ v^{(1)}(x,\theta) \\ w^{(1)}(x,\theta) \end{Bmatrix} = \sum_{m=0}^{2N} \begin{Bmatrix} u^{(0)}_m(x) \\ v^{(0)}_m(x) \\ w^{(0)}_m(x) \\ u^{(1)}_m(x) \\ v^{(1)}_m(x) \\ w^{(1)}_m(x) \end{Bmatrix} g_m(\theta), \tag{16}$$

where N ($= N_u$ or N_v or N_w), is the number of terms in the relevant series. The external loads q_u, q_v and q_w are also expanded as

$$\begin{Bmatrix} q_u(x,\theta) \\ q_v(x,\theta) \\ q_w(x,\theta) \end{Bmatrix} = \sum_{m=0}^{2N_q} \begin{Bmatrix} q_m^u(x) \\ q_m^v(x) \\ q_m^w(x) \end{Bmatrix} g_m(\theta). \tag{17}$$

The functions $g_m(\theta)$ are

$$g_m(\theta) = \begin{cases} \cos(nm\theta) & m = 0,1,\ldots,N, \\ \sin(n(m-N)\theta) & m = N+1,\ldots,2N, \end{cases} \tag{18}$$

n denoting the characteristic circumferential wave number. Recourse to a characteristic wave number makes it possible, in some cases, to substantially reduce the number of terms in the Fourier series (Narasimhan and Hoff, 1971). For general cases, in which all terms are significant, it is necessary to let $n = 1$ and N sufficiently large for accurate representation of u, v and w.

Minimizing the errors in the governing equations due to the truncation of the Fourier series by applying the Galerkin procedure with $\cos(\cdot)$ and $\sin(\cdot)$ as weighting functions, we obtain the following nonlinear and linear ordinary differential equations for the nonlinear pre-buckling and the linear buckling states, respectively:

$$\begin{aligned} \Phi_r^q(\mathbf{z}^{(0)};x) &= \oint \phi_r^{(0)}(u^{(0)}(x,\theta), v^{(0)}(x,\theta), w^{(0)}(x,\theta)) g_q(\theta)\,\mathrm{d}\theta, \quad q = 0,1,\ldots,2N, \;\; r = 1,2,3; \\ \Psi_r^q(\mathbf{z}^{(1)};x) &= \oint \phi_r^{(1)}(u^{(0)}(x,\theta), v^{(0)}(x,\theta), w^{(0)}(x,\theta), u^{(1)}(x,\theta), v^{(1)}(x,\theta), w^{(1)}(x,\theta)) g_q(\theta)\,\mathrm{d}\theta, \\ & \qquad q = 0,1,\ldots,2N, \;\; r = 1,2,3, \end{aligned} \tag{19}$$

where $\mathbf{z}^{(0)}$ or $\mathbf{z}^{(1)}$ is unknown vector function, defined by

$$\mathbf{z} = \{u_0,\ldots,u_{2N_u}, v_0,\ldots,v_{2N_v}, w_0,\ldots,w_{2N_w}, \xi_0,\ldots,\xi_{2N_w}\}^{\mathrm{T}}. \tag{20}$$

The new function ξ is defined as $\xi = w_{,xx}$. Finally, using the finite-difference scheme, Eqs. (19) yield

$$\begin{aligned} &[\mathbf{K}^{(0)}(\bar{\mathbf{z}}^{(0)}, P)]\bar{\mathbf{z}}^{(0)} = \mathbf{0}, \\ &[\mathbf{K}^{(1)} + \lambda \mathbf{G}^{(1)}(\bar{\mathbf{z}}^{(0)}) + \lambda^2 \overline{\mathbf{G}}^{(1)}(\bar{\mathbf{z}}^{(0)})]\bar{\mathbf{z}}^{(1)} = \mathbf{0}, \end{aligned} \tag{21}$$

where $\bar{\mathbf{z}}$ are the values of the unknowns vector function ($\mathbf{z}$) in the finite-difference scheme, $\mathbf{K}^{(0)}$ is the pre-buckling stiffness matrix consisting of nonlinear algebraic operators, $\mathbf{K}^{(1)}$ is the linear stiffness matrix. $\mathbf{G}^{(1)}$ and $\overline{\mathbf{G}}^{(1)}$ are the geometric matrices of the buckling state, functions of the linear and nonlinear state ($\bar{\mathbf{z}}^{(0)}$), respectively. P is the load level at which the eigenproblem is treated, and λ is the eigenvalue parameter. The buckling load is then λP.

Obtaining the nonlinear bifurcation point $(\lambda P, \bar{\mathbf{z}}^{(1)})$ is an iterative procedure. The initial load level $P = 1$ is assigned, then the nonlinear pre-buckling state, $\bar{\mathbf{z}}^{(0)}$, is obtained using the nonlinear equation (21a). Substituting $\bar{\mathbf{z}}^{(0)}$ in Eq. (21b), we obtain the eigenvalue (λ) and the eigenvector ($\bar{\mathbf{z}}^{(1)}$). The process is repeated for different load levels, calculating by the following Eq. (22), until λ converges to 1, when the buckling occurs. A new algorithm is suggested for the iterative process:

$$P^i = P^{i-1}\left(1 + \frac{\lambda - 1}{\beta}\right), \tag{22}$$

where i denotes the iteration number and β is the convergence factor. Note that this iteration process converges for any $\beta > 1$.

4. Results and discussion

A general-purpose computer code NBCS (*N*onlinear *B*uckling of *C*onical *S*hells), written for the outlined procedure. The object of the study is an isotropic conical shell under axial compression with data as follows: modulus of elasticity $E = 1.4040 \times 10^{11}\ \mathrm{N/m^2}$, Poisson's ratio $v = 0.2$, radius at $x = 0$ is $R_1 = 1.27$ m, and thickness $h = 0.0127$ m ($R_1/h = 100$). The problem to be solved is the effect of the nonlinear pre-buckling deformations on the bifurcation state as a function of the cone vertex half-angle, (α).

The first example concerns a cylindrical shell ($\alpha = 0$) with the following clamped–clamped boundary conditions: CC1 $(N_{xx} = -\overline{N}_{xx}, N_{x\theta} = 0, w = w_{,x} = 0)$ at $x = 0$ and CC4 $(u = v = w = w_{,x} = 0)$ at $x = L$ ($= 2.54$ m).

The entire nonlinear behavior was obtained for the cylindrical shell and Donnell's shell theory by the code of Sheinman and Jabareen (2005). The nonlinear behavior of the axial compression vs. the average end shortening, $e_{av} = -\int_A u_{,x}\,\mathrm{d}A/(2\pi R_1 L)$ is shown in Fig. 2. The dashed and solid lines are the equilibrium paths obtained with large and small arc-length parameters, respectively, and their intersection is the nonlinear bifurcation point. The present NBCS code for linear and nonlinear pre-buckling (using Donnell's shell theory) yields buckling at $\overline{N}_{xx} = 10,525\ \mathrm{kN/m}$ (namely, $\overline{N}_{xx,\mathrm{cl}}$) and $\overline{N}_{xx} = 9767\ \mathrm{kN/m}$ (namely, $\overline{N}_{xx,\mathrm{bif}}$), respectively; the second result coinciding with bifurcation point obtained by the entire nonlinear behavior (given by the intersection of the equilibrium paths). The reason for its being lower than the first is the decrease of the stiffness near the bifurcation point, as shown in Fig. 3.

The effect of the nonlinear pre-buckling state is more pronounced in the buckling mode. The buckling mode for linear pre-buckling (LPB) and nonlinear pre-buckling (NPB) is shown in Fig. 4(a) and (b), respectively, and the mode along the axial coordinate for $\theta = 0$ in Fig. 5. It is seen that the nonlinear effect produces for a significant wave amplitude close to the load edge for u and w displacements, while that the torsion effect (see v displacement) is significantly reduced.

Convergence of the iterative procedure for λ in Eq. (21), which depends on the parameter β, is shown in Fig. 6. $\overline{N}_{xx}$ is the applied axial force (the load level P^{i-1} in Eq. (21a)), and $\overline{N}^*_{xx}$ is the axial load obtained by

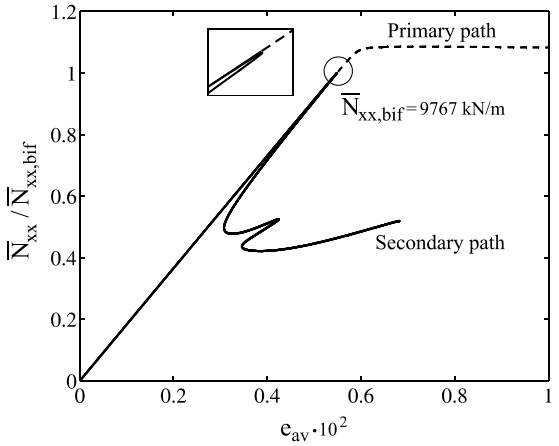

Fig. 2. Applied axial load vs. average end shortening—primary and secondary equilibrium paths.

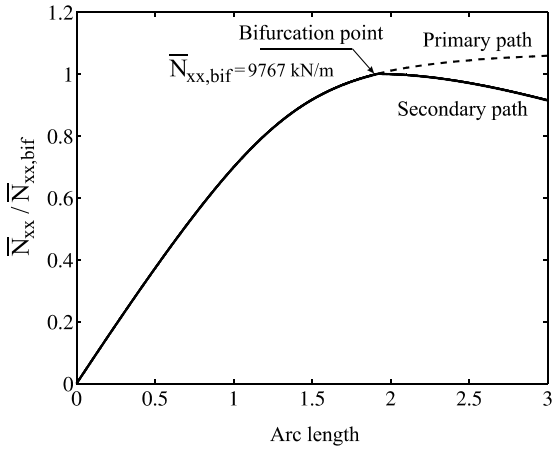

Fig. 3. Applied axial load vs. arc-length parameter.

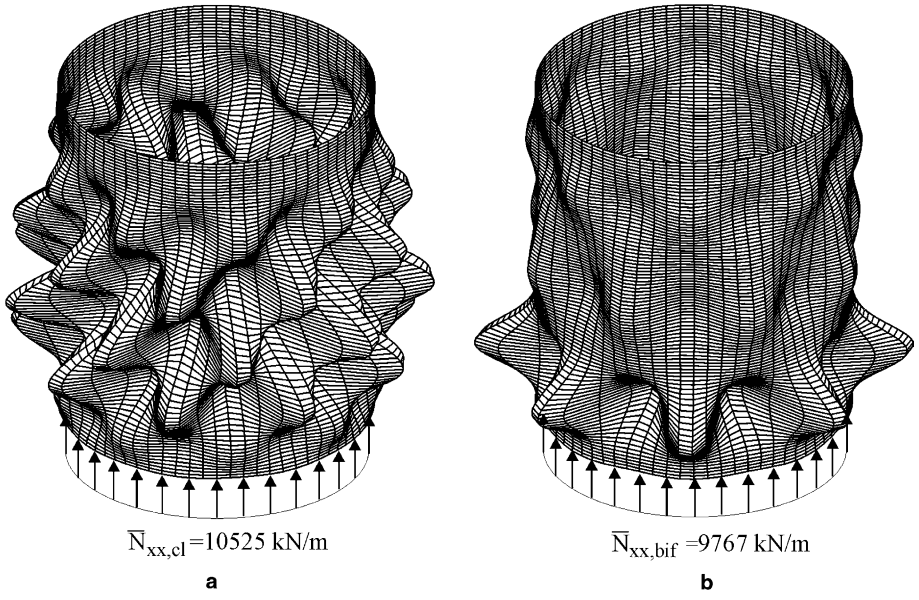

Fig. 4. Cylindrical buckling modes for linear and nonlinear pre-buckling states: (a) LPB and (b) NPB.

Eq. (22), ($\equiv P^i$). It is observed that for small values of β a small number of iterations is needed to obtain $\lambda = 1$ and that the calculated points are located on the same smooth curve, obtained by large value of β. Hence, the only condition for β is to be greater than unity.

The accuracy of Donnell's theory was checked by comparison with an accurate theory—Sanders', and a more accurate one—Timoshenko's. The results, summarized in Table 1, show that Donnell's theory can be used with very good agreement, especially for short cylindrical shells. Furthermore, it is found that for both LPB and NBP, the more accurate theory yields a lower buckling load.

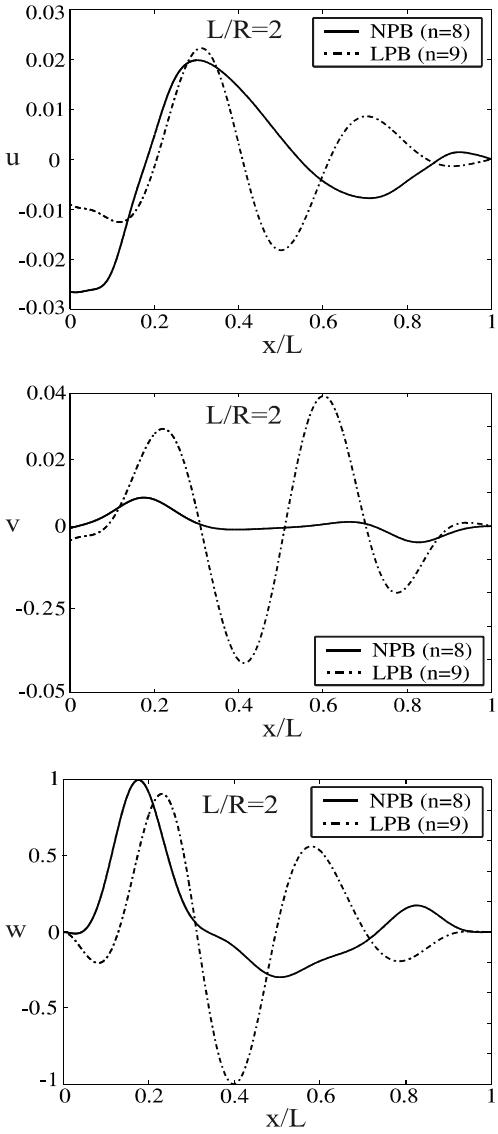

Fig. 5. Buckling mode for $L/R = 2.0$, axial (u), circumferential (v) and normal (w) displacements.

The effect of the length:radius (L/R) ratio on the buckling load is shown in Fig. 7. It is seen that for long shells, the difference between the LPB and NPB cases (with regard to Timoshenko's theory) decreases, and that Donnell's theory is no longer satisfied.

The second example concerns shells with $\alpha \neq 0$. In Fig. 8 the buckling load under axial compression is plotted vs. the L/R_1 ratio for $\alpha = 5°$. It can be seen that the discrepancy between the three theories is very small and it was found to vanish at $\alpha > 10°$. However, the difference between the LBP and NPB states is still significant. Results against L/R_1 ratio at different α's are shown in Fig. 9. It is seen that for $\alpha > 30°$ and $L/R_1 > 5$, the buckling load is independent of L/R_1. Furthermore, as expected, for $\alpha = 90°$ (annular plate) the LPB results are identical with the NPB's.

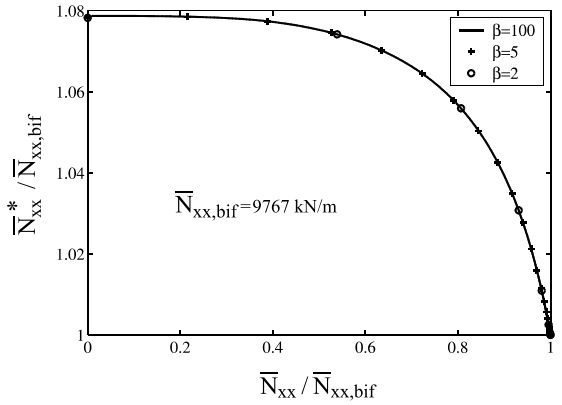

Fig. 6. Nonlinear eigenvalue convergence curve.

Table 1
Axial buckling load of cylindrical shell ($L/R = 2.0$)

	LPB (kN/m)	NPB (kN/m)
Donnell	10,525	9767
Sanders	10,473	9734
Timoshenko	10,386	9679

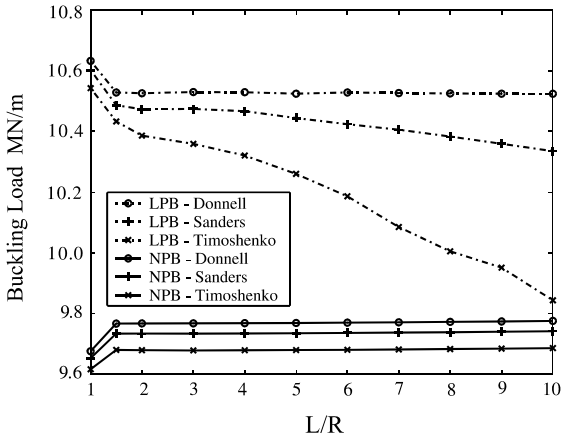

Fig. 7. Linear (LPB) and nonlinear (NPB) buckling load of cylindrical shell ($\alpha = 0°$) according to shell theories.

In view of the pronounced effect of the in-plane boundary conditions as shown by Goldfeld et al. (2003), nonlinear vs. linear pre-buckling was checked out for simply supported boundary condition: SS1 $(N_{xx} = -\overline{N}_{xx}, N_{x\theta} = w = M_{xx} = 0)$ or SS3 $(N_{xx} = -\overline{N}_{xx}, v = w = M_{xx} = 0)$ at $x = 0$, and SS4 $(u = v = w = M_{xx} = 0)$ at $x = L = 2.54$ m. Results are shown in Fig. 10. It is seen that for SS3–SS4, the effect of the nonlinear pre-buckling is pronounced, while for SS1–SS4 is insignificant. Furthermore, $N_{x\theta} = 0$ yields a lower buckling load than $v = 0$.

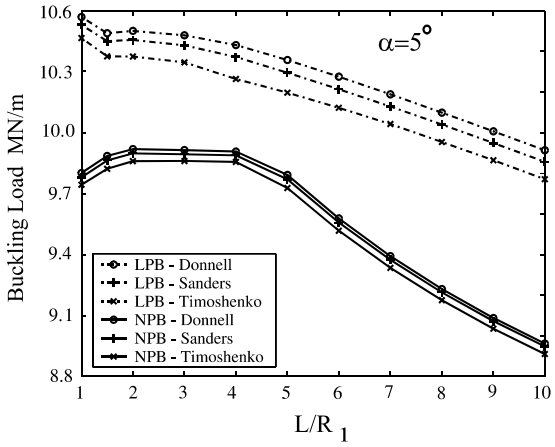

Fig. 8. Linear (LPB) and nonlinear (NPB) buckling load of conical shell ($\alpha = 5°$) according to shell theories.

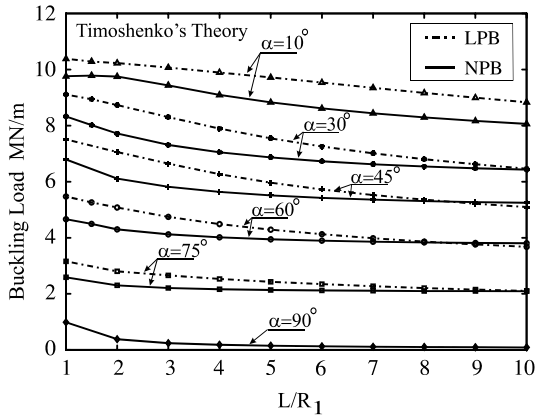

Fig. 9. Effect of vertex half-angle on linear (LPB) and nonlinear (NPB) buckling load of conical shells.

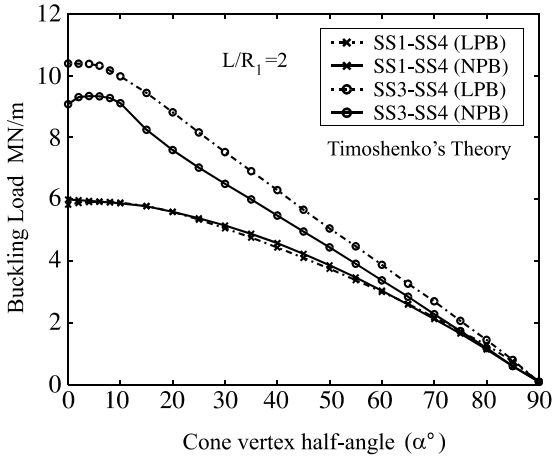

Fig. 10. Effect of in-plane boundary conditions on buckling load for simply supported conical shell.

5. Concluding remarks

A procedure for the buckling behavior under the effect of the nonlinear pre-buckling deformations is presented for conical shells. The buckling load was examined via three theories: Donnell's, Sanders' and Timoshenko's.

- The nonlinear pre-buckling deformations affect the critical buckling load and more significantly the buckling mode. For structures characterized by softening behavior, the nonlinear pre-buckling leads to a buckling load lower than the classical one.
- The longer the shell the weaker the effect of the nonlinear pre-buckling deformations.
- The nonlinear pre-buckling effect strongly depends on the in-plane boundary conditions.
- The discrepancy between the shell theories is observed only for cylindrical shells and for conical shells with small vertex half-angle.
- Finally, for structures characterized by a limit point, the suggested procedure is very efficient and economical: it predicts the actual buckling load and mode with no need for covering the entire nonlinear pattern.

Acknowledgements

This study was partially supported by the fund for Promotion of Research at the Technion. The authors are indebted to Ing. E. Goldberg for editorial assistance.

References

Baruch, M., Harari, O., Singer, J., 1970. Low buckling loads of axially compressed conical shells. J. Appl. Mech. 37 (2), 384–392.
Brendel, B., Ramm, E., 1980. Linear and nonlinear stability analysis of cylindrical shells. Comp. Struct. 12 (4), 549–558.
Brush, D.O., 1980. Prebuckling rotations and cylinder buckling analysis. J. Engng. Mech. Div. Proc. ASCE 106 (EM2), 225–232.
Chang, S.C., Chen, J.J., 1986. Effectiveness of linear bifurcation analysis for predicting the nonlinear stability limits of structures. Int. J. Num. Meth. Engng. 23 (5), 831–846.
Donnell, L.H., 1933. Stability of thin-walled tubes under torsion. NACA TR-479.
Famili, J., 1965. Asymmetric buckling of finitely deformed conical shells. AIAA J. 3 (8), 1456–1461.
Goldfeld, Y., Arbocz, J., 2004. Buckling of laminated conical shells given the variations of the stiffness coefficients. AIAA J. 42 (3), 642–649.
Goldfeld, Y., Sheinman, I., Baruch, M., 2003. Imperfection sensitivity of conical shells. AIAA J. 41 (3), 517–524.
Narasimhan, K.Y., Hoff, N.J., 1971. Snapping of imperfect thin-walled circular cylindrical shells of finite length. J. Appl. Mech. 38 (1), 162–171.
Pariatmono, N., Chryssanthopoulos, M.K., 1995. Asymmetric elastic buckling of axially compressed conical shells with various end-conditions. AIAA J. 33 (11), 2218–2227.
Sanders, J.L., 1963. Nonlinear theories for thin shells. Quart. J. Appl. Math. 21 (1), 21–36.
Seide, P., 1956. Axisymmetrical buckling of circular cones under axial compression. J. Appl. Mech. 23 (4), 625–628.
Sheinman, I., Goldfeld, Y., 2001. Buckling of laminated cylindrical shell in terms of different theories and formulations. AIAA J. 39 (9), 1773–1781.
Sheinman, I., Goldfeld, Y., 2003. Imperfection sensitivity of laminated cylindrical shells according to different shell theories. J. Eng. Mech. ASCE 129 (9), 1048–1053.
Sheinman, I., Jabareen, M., 2005. Post-buckling of laminated cylindrical shells in different formulations. AIAA J. 43 (5), 1117–1123.
Simitses, G.J., Shaw, D., Sheinman, I., 1985. The accuracy of Donnell's equation for axially-loaded imperfect orthotropic cylinders. Comp. Struct. 20 (6), 939–945.
Singer, J., 1962. The effect of axial constraint on the instability of thin conical shells under external pressure. J. Appl. Mech. 29 (1), 212–214.

Singer, J., 1965. Buckling of circular conical shells under uniform axial compression. AIAA J. 3 (5), 985–987.
Spagnoli, A., 2003. Koiter circles in the buckling of axially compressed conical shells. Int. J. Solid Struct. 40, 6095–6109.
Timoshenko, S., Gere, J.M., 1961. Theory of Elastic Stability. McGraw-Hill, New York.
Tong, L., 1994. Buckling load of composite conical shells under axial compression. J. Appl. Mech. 61 (3), 718–719.
Zhang, G.Q., 1993. Stability analysis of anisotropic conical shells. Ph.D. dissertation, Faculty of Aerospace Engineering, Delft University of Technology, Delft University Press, Delft, The Netherlands.